

Lamprey Hemoglobin

STRUCTURAL BASIS OF THE BOHR EFFECT*

Received for publication, July 23, 1999, and in revised form, December 22, 1999

Yang Qiu^{‡§}, David H. Maillett[¶], James Knapp^{||**}, John S. Olson[¶], and Austen F. Riggs^{‡ ††}

From the [‡]Section of Neurobiology, School of Biological Sciences and Institute for Molecular and Cell Biology, University of Texas, Austin, Texas 78712-1064, the [¶]Department of Biochemistry and Cell Biology and the Keck Center for Computational Biology, Rice University, Houston, Texas 77005-1892, and the ^{||}Department of Chemistry and Biochemistry, University of Texas, Austin, Texas 78712-1167

Lampreys, among the most primitive living vertebrates, have hemoglobins (Hbs) with self-association and ligand-binding properties very different from those that characterize the $\alpha_2\beta_2$ tetrameric Hbs of higher vertebrates. Monomeric, ligated lamprey Hb self-associates to dimers and tetramers upon deoxygenation. Dissociation to monomers upon oxygenation accounts for the cooperative binding of O₂ and its pH dependence. Honzatko and Hendrickson (Honzatko, R. B., and Hendrickson, W. A. (1986) *Proc. Natl. Acad. Sci. U. S. A.* 83, 8487–8491) proposed that the dimeric interface of the Hb resembles either the $\alpha_1\beta_2$ interface of mammalian Hbs or the contacts in clam Hb where the E and F helices form the interface. Perutz (Perutz, M. F. (1989) *Quart. Rev. Biophys.* 2, 139–236) proposed a version of the clam model in which the distal histidine swings out of the heme pocket upon deoxygenation to form a bond with a carboxyl group of a second monomer. The sedimentation behavior and oxygen equilibria of nine mutants of the major Hb component, PMII, from *Petromyzon marinus* have been measured to test these models. The results strongly support a critical role of the E helix and the AB corner in forming the subunit interface in the dimer and rule out the $\alpha_1\beta_2$ model. The pH dependence of both the sedimentation equilibrium and the oxygen binding of the mutant E75Q indicate that Glu⁷⁵ is one of two groups responsible for the Bohr effect. Changing the distal histidine 73 to glutamine almost completely abolishes the self-association of the deoxy-Hb and causes a large increase in O₂ affinity. The recent x-ray crystallographic determination of the structure of deoxy lamprey Hb, reported after the completion of this work (Heaslet, H. A., and Royer, W. E. (1999) *Structure* 7, 517–526), shows that the dimer interface does involve the E helix and the AB corner, supporting the measurements and interpretations reported here.

* This work was supported by National Science Foundation Grants MCB 951179 and 972385 (to A. F. R.), National Institutes of Health Grants GM 35649 and HL 47020 (to J. S. O.), and National Institutes of Health Biotechnology Training Grant T32-GM08362. Portions of this paper are based on a Ph.D. dissertation of Y. Qiu at the University of Texas at Austin, December, 1997. A preliminary account of the results has been presented (1). The costs of publication of this article were defrayed in part by the payment of page charges. This article must therefore be hereby marked "advertisement" in accordance with 18 U.S.C. Section 1734 solely to indicate this fact.

The nucleotide sequence(s) reported in this paper has been submitted to the GenBank™/EBI Data Bank with accession number(s) AF248645.

§ Present address: Functional Genomics Department, Lawrence Berkeley National Laboratory, 1 Cyclotron Rd., MS84-171, Berkeley, CA 94720.

** Present address: Dept. of Biochemistry and Molecular Biology, University of Massachusetts Medical School, Worcester, MA 01655.

†† To whom correspondence should be addressed. Tel.: 512-471-1585; Fax: 512-471-9651; E-mail: riggs@uts.cc.utexas.edu.

Lampreys and hagfish, the most primitive living vertebrates, have hemoglobins (Hbs)¹ distinct from those of all others in the class. Indeed, the low isoelectric points of the Hbs caused Svedberg and Eriksson (2) to identify them with invertebrate Hbs for which they had revived the term *erythrocrucorin*.² They found the Hbs to be monomeric, like myoglobins, rather than the tetramers characteristic of other vertebrates. However, Wald and Riggs (6) found that oxygen equilibria of lamprey (*Petromyzon marinus*) Hb were strongly pH-dependent (Bohr effect), a surprising result at the time because oxygen equilibria of the monomeric myoglobins were pH-independent. Furthermore, they found that the oxygen equilibrium at pH 6.8 was slightly cooperative, with a Hill coefficient of 1.2, but dismissed this result as an artifact because cooperativity is impossible with monomeric Hbs. Briehl (7) resolved this paradox by showing that deoxygenated lamprey Hb self-associates. Protonation accompanying the association accounts for the Bohr effect of O₂ binding. Behlke and Scheler (8) showed with sedimentation velocity measurements that ligated Hb from a similar species of lamprey (*Lampetra fluviatilis*) also self-associates, but only at low pH. Although the metHb was found to be monomeric, addition of metHb ligands such as azide or cyanide causes dimer formation at low pH (9). This property, oxidation-induced dissociation and ligand-dependent reassociation, absent in other vertebrate Hbs, but found in the Hbs of organisms of five invertebrate phyla, is another indication of the functional relationship of lamprey and invertebrate Hbs (10).

Andersen and Gibson (11, 12) showed by kinetic analysis of ligand binding by the Hb of *P. marinus* that the results could be accurately described by a model in which protonation of a single site per monomer with pK = 6.0 accompanied the formation of dimers of low O₂ affinity. There was no need to include self-association beyond the dimer, so they concluded that higher aggregates may not be physiologically important. This conclusion was reinforced by sedimentation equilibria of the deoxy-Hb which indicated only very weak dimer-tetramer association. However, the conclusion that tetramers are physiologically insignificant was based on extrapolation of kinetic and sedimentation measurements at 10–60 μ M concentration to millimolar concentrations. Dohi *et al.* (13) extended the sedimentation measurements to concentrations of 3 mM with Hb from another species of lamprey, *Entosphenus japonicus*. Their results suggested that as much as 85% of the deoxy-Hb within red cells of this species would be tetrameric. The amino acid composition (13) of *E. japonicus* globin is virtually identi-

¹ The abbreviations used are: Hb, hemoglobin; PCR, polymerase chain reaction; bp, base pair(s).

² Lankester (3) designated "erythrocrucorin" to include all red blood proteins of invertebrates, but soon abandoned the term (4) after "hemoglobin," first proposed by Hoppe-Seyler (5), came into use.

TABLE I
Synthetic oligonucleotides

No.	Sequence ^a	Description (strand)
1	CTCGAGTCTAGATTTTFTTTTFTTTT	Oligo(dT) with <i>Xba</i> I adapter
2	GCNGCNGARAARACNAARATHMG	PMII-degenerate primer (numbers 13–20(+))
3	GTCGACCTGGAAGCTTTTGGCGTG	PMII-GSP1–5' (numbers 105–112)(–)
4	GAGGTCTCATAATTGGAGTACACG	PMII-GSP2–5' (numbers 25–33)(–)
5	TTCTGACTCCCTTCGACGGATC	PMII-5' non-coding sequence (–54 to –33)
6	ATGCCTATCGTCGACACNGGAAGCG	PMII-NH ₂ -terminal (numbers 1–8(+))

^a N: (A, C, G, T), R: puRine (A, G), H: (A, C, T), M (A, C). Numbers in the right-hand column refer to amino acids in the coding region or to base pairs in non-coding regions. The plus and minus signs refer to strand sense.

cal with that of *P. marinus*, which suggests that very few differences in amino acid sequence exist.

The nature of the functionally important dimer of lamprey Hb has been uncertain. Although four different crystal forms of deoxy lamprey Hb have been identified (14), none proved amenable to structure determination. Honzatko and Hendrickson (15) proposed on the basis of model building that the interface in the deoxy-Hb dimer might resemble either the $\alpha_1\beta_2$ interface characteristic of tetrameric vertebrate Hbs or that in the clam *Scapharca* in which the interface involves the E/F and A/B helices. Perutz (16) noted that the pH dependence of O₂ binding suggested participation of histidyl residues. Since the only two histidines present are the proximal and distal residues on each side of the heme, he proposed that the distal residue swings out of the heme pocket upon deoxygenation to form an electrostatic link with a carboxyl group of another monomer. This would raise the p*K* of the histidine and explain the Bohr effect.

The goal of the present studies was to construct mutant Hbs by site-directed mutagenesis and measure the sedimentation and O₂ binding properties in order to distinguish between two interface models. After completion of the experimental work, the x-ray structure of one form of dimeric deoxy-Hb of the adult has been reported which shows that the subunit interface is between the E helices and AB corners (17). Our work now serves to confirm the functional significance of this structural feature (17).

MATERIALS AND METHODS

Blood Collection—Adult and larval lampreys (*P. marinus*) were obtained from the Hammond Bay Biological Station, Millersburg, MI. Blood from decapitated lampreys was collected in ice-cold 1 mM Tris-HCl, pH 7.5, 250 mM NaCl, with a small amount of heparin. Packed red cells, washed twice with this buffer, were frozen with liquid nitrogen and stored at –80 °C.

mRNA and cDNA—The mRNA from adults was extracted with the Fast Track mRNA Isolation Kit, Version 3.5 (Invitrogen, San Diego, CA). mRNA (7 μ l, 10 μ g) was mixed with 3 μ l of diethylpyrocarbonate-treated deionized water (dH₂O) (3 μ l) containing 500 ng of an oligo(dT) 28-mer containing an *Xba*I site at the 5' end (number 1, Table I). The water was prepared by adding 100 μ l of diethylpyrocarbonate (Sigma number D5758) to 100 ml of deionized water and shaking at 37 °C overnight. The annealing reaction was carried out by incubation of the mixture at 65 °C for 5 min, followed by cooling on ice. The following components were then added: RNasin (1 μ l, 40 units/ μ l, Promega), 8 μ l of 2.5 mM dNTP mixture, 10 μ l of 5 \times reverse transcription buffer (U. S. Biochemicals), 5 μ l 0.1 M dithiothreitol (Life Technologies, Inc.), 14 μ l diethylpyrocarbonate-dH₂O, and 2 μ l of reverse transcriptase (100 units/ μ l Moloney murine leukemia virus). After incubation for 1 h at 37 °C, 5 μ l of 3 M sodium acetate and 125 μ l of 100% ethanol were added. After precipitation overnight at –20 °C, the resulting pellet was dissolved in 20 μ l of diethylpyrocarbonate-dH₂O.

Amplification and Cloning of cDNA for Adult Globin—The cDNA was amplified by the polymerase chain reaction (PCR) using oligo(dT) with an *Xba*I site (number 1, Table I) and a 3,072-fold redundant oligomer (number 2, Table I) based on residues 13–20 of both components PMII and PMIII of Refs. 18 and 19. PMII corresponds to component V (Ref. 20) used in crystallographic studies. The 100- μ l PCR reaction mixture contained 2 μ l of the mRNA-cDNA duplex from the reverse transcription, 1 \times Assay Buffer A from Fisher Biotech (10 \times Assay Buffer A: 100 mM Tris-HCl, pH 8.3, at 25 °C, 500 mM KCl, 15 mM

MgCl₂, and 0.01% gelatin), 0.1 mg/ml bovine serum albumin, 200 μ M dNTP, 100 pmol of each primer, and 2.5 units of *Taq* polymerase (Fisher Biotech). Denaturation at 94 °C for 5 min was followed by 30 cycles of 1 min each at 94 °C for denaturing, 48 °C for annealing, 72 °C for elongation, and a final 15 min at 72 °C for complete elongation. Analysis of the PCR product by agarose gel electrophoresis showed a single band of 600 bp which was isolated by "Gene Clean" II Kit (BIO-101 Inc., Vista, CA) and cloned into the *Sma*I site of pUC19 and sequenced by the dideoxy chain termination method by using Sequenase Kit Version 2.0 (U. S. Biochemical, Cleveland, OH). 5' Rapid Amplification of 5' cDNA End Kit (Life Technologies, Inc.) was used to amplify the 5' coding and untranslated sequences of the globin cDNA. Primer GSP1–5' (number 3, Table I), complementary to the cDNA of PMII, was used in the reverse transcription reaction, and an oligo(dC) anchor sequence was added to the 5' end of the cDNA using terminal deoxynucleotidyl transferase supplied in the RACE Kit. GSP1–5' corresponds to residues 105–112 which are identical in PMI, II, and III (18, 19). A nested PCR amplification was carried out using GSP2–5' (Table I, number 4) and a deoxyinosine-containing Anchor Primer (AP) provided with the kit. The second PCR product was analyzed by gel electrophoresis and cloned into pUC19 for sequencing. After obtaining the 5' non-coding sequences of the cDNA, oligomer number 5, constructed to correspond to the 5' non-coding region of both PMII and PMIII, together with oligo(dT), made amplifications of the complete cDNA sequences possible.

The amplified cDNA products were blunt-ended by the addition of 1 μ l of DNA Polymerase I Large Fragment (Klenow, 1 unit/ μ l, Promega) and incubating for 1 h at 37 °C. The amplified products were eluted after electrophoresis on a 1.0% agarose gel with the Gene Clean II Kit (BIO 101). Ligation with pUC19 cut with *Sma*I to give blunt ends was performed with the TaKaRa Ligation Kit (TaKaRa Biochemicals). The ligated product was cloned with MAX efficiency DH5 α competent cells from Life Technologies, Inc. (catalog number 18258-012). Positive plasmids were sequenced by the Sanger dideoxy termination method using the Sequenase Kit Version 2.0 (U. S. Biochemicals).

Expression—Plasmid pHE7, provided by Dr. Chien Ho, Department of Biological Sciences, Carnegie Mellon University, Pittsburgh, PA, co-expresses *Escherichia coli* methionine aminopeptidase and human Hb α and β subunits (21). The expressed methionine aminopeptidase removes the NH₂-terminal methionine. The α and β subunit cDNAs were replaced with cDNA for lamprey globin. This was done by digesting pHE7 completely with *Nsi*I and then partially digesting with *Nde*I to yield a 5.91-kilobase fragment that was purified by electrophoresis on a 0.7% agarose gel. The fragment was cut out and eluted from the gel with Gene Clean Kit (BIO 101, Inc.). The cDNA for globin component PMII was generated by PCR of the cDNA with two terminal primers (numbers 1001 and 1005, Table II) which are complementary to the 5' and 3' ends of the PMII cDNA and contain *Nde*I and *Nsi*I sites, respectively. The resulting PCR product was ethanol precipitated, digested with *Nde*I and *Nsi*I, and run on an agarose gel; the 450-bp product was eluted with the Gene Clean Kit and ligated to the 5.91-kilobase fragment of pHE 7 with the TaKaRa Ligation Kit (TaKaRa Biochemicals, Inc.). The 6.36-kilobase product (pHE7-PMHb) can coexpress both *E. coli* methionine aminopeptidase and the lamprey globin. The ligation product was used to transform JM109 competent cells (Promega, Madison, WI) and positive clones with inserts were selected. JM109 clone number 4 was used to express the lamprey PMII globin. The cDNA-derived amino acid sequence for clone 4 was identical to that of PMII (19) except that position 86 was Val instead of Ala and is therefore designated PMII'. The recent crystallographic studies (17) indicate that this difference is unlikely to have any significant functional effect. All the mutagenesis utilized this clone. A single colony of JM109 cells with the pHE7 plasmid containing the cDNA for the globin was used to inoculate 2 ml of LB broth containing 100 μ g/ml ampicillin and grown for 8 h at 37 °C. A 160- μ l aliquot of the culture was added to 40 ml of LB

TABLE II
Synthetic oligonucleotides for site-directed mutagenesis

The underlined codons in the middle column refer to the changed codon for the site-directed mutagenesis except the TTA in oligomer 1005 which designates the stop codon. The italicized sequences refer to the restriction site *Nsi*I or *Nde*I. Numbers in the right-hand column refer to amino acids in the coding region for PMII.

No.	Sequence	Description (strand)
1001	AAGCAATCCATATGCCTATCGTCGACACTG	PMII NH ₂ -terminal primer with <i>Nde</i> I site (+)
1005	TGAATAGCCATGCATGTTTCATTAGTAGGC	PMII COOH-terminal primer with <i>Nsi</i> I site (-)
1006	GGGGAAGAACTGCTGAGCAGC	E50Q (numbers 47-53(-))
1007	CCTCTCGGCCCTGCCAGCGCAC	H73Q (numbers 70-76(-))
1008	TTCCAGGTCAACCCCCAGTAC	D112N (numbers 109-115(+))
1009	TGGCAGCCAGAGGATCATC	E75Q (numbers 72-78(+))
1011a	CATCGACGCCGTCAACGATG	N79D (numbers 77-84(+))
1012	AGGATCATCCACGCCGTCAAC	N79H (numbers 76-82(+))
1013	AGAGTCTCGTGATTGGAGTA	Y30H (numbers 27-33(-))
1014a	CCACACCAGAGGTCTTATAATTG	E31K (numbers 28-36(-))
1015	GACACCGAGGAGATGAGCATG	K93E (numbers 90-96(+))

with ampicillin and grown overnight at 37 °C. A 10-ml aliquot of this culture was then added to 1 liter of TB with ampicillin in a 4-liter flask and shaken at 30 °C for about 5 h until the absorbance at 600 nm reached 1.0. Glucose (10 g/liter) and δ -aminolevulinic acid (20 mg/liter) was then added. Expression of Hb was induced by adding isopropyl-1-thio- β -D-galactopyranoside to a concentration of 0.2 mM and continuing the incubation for 5 h at 30 °C. The centrifuged pellet from the culture was resuspended in 20 ml of 50 mM Tris-HCl, 1 mM EDTA, pH 8.0, frozen in liquid N₂, and stored at -80 °C.

Mutagenesis—The “Megaprimer” method of Sarkar and Sommer (22) was used. Nine internal oligomers were constructed in each of which a single nucleotide change was made (Table II). The procedure, described here for one mutant, as an example, utilizes two successive PCRs. Oligomers 1006 and 1001 (Table II) were used in the first PCR to amplify part of the cDNA sequence with incorporation of the altered codon in oligomer 1006. Oligomer 1001 contains a *Nde*I restriction site. The 100- μ l PCR reaction mixture contained 50 ng of plasmid DNA from JM109#4, 1 \times Assay buffer from Fisher Biotech (10 \times buffer: 100 mM Tris-HCl, pH 8.3, at 25 °C, 500 mM KCl, 15 mM MgCl₂, and 0.01% gelatin), 0.1 mg/ml bovine serum albumin, 200 μ g/ml dNTP, 100 pmol of each primer, and 2.5 units of *Taq* polymerase (Fisher Biotech). Denaturation at 94 °C for 5 min was followed by 30 cycles (1 min each) at 94 °C denaturing, 54 °C for elongation, and a final 15 min at 72 °C for complete elongation. The amplified 170-bp product was electrophoresed in a 1.5% agarose gel and eluted with the QIA quick Gel Extraction Kit (QIAGEN, Inc.). The 170-bp product was used as the megaprimer in the second PCR with oligomer 1005 (Table II). A good yield required the template DNA in the second PCR to be increased from 0.2 (22) to 2 μ g (23, 24). The 100 μ l for the second PCR contained 2 μ g of plasmid DNA (JM109#4), 1 \times Assay Buffer from Fisher Biotech, 0.1 mg/ml bovine serum albumin, 200 μ M dNTP, 50 pmol each of the megaprimer and a terminal primer 1001 or 1005, and 2.5 units of *Taq* polymerase (Fisher). After denaturation at 95 °C for 5 min, 6 cycles were carried out at 94 °C for 1 min and 72 °C for 2 min *without* the terminal primer which was then added, and 28 cycles of 94 °C (1 min), 52 °C (2 min), and 72 °C (2 min) were performed. The resulting 450-bp product was digested with *Nde*I and *Asi*I and inserted between these sites in the pHE7 expression vector.

Purification—JM109 cells from a 1-liter culture overexpressing the recombinant Hbs were lysed on ice for 5 h in an 80-ml solution of 50 mM Tris-HCl, pH 8.0, 1 mM EDTA, 0.5 mM dithiothreitol, 40 units/ml DNase I, 3 units/ml RNase A, and 2 mg/ml lysozyme. The lysate was then frozen in liquid nitrogen and thawed twice to break the cells. Cell debris was removed by centrifugation at 12,000 rpm, 30 min (Sorvall rotor SS34). The reddish supernatant was saturated with CO, made 55% saturated with ammonium sulfate, and stirred on ice for 2 h. The precipitate was discarded, and the supernatant was made 95% saturated with ammonium sulfate and stirred for 2 h on ice. The pellet, obtained by centrifugation, was resuspended in a minimum volume of 20 mM Tris-HCl, 1 mM EDTA, pH 8.0, and dialyzed (Spectropor tubing with 12,000–14,000 M_r cutoff) against 20 mM Tris-HCl, 1 mM EDTA, pH 8.0, for at least 36 h at 4 °C with three changes of buffer. The sample was applied to a DEAE-Sepharose CL-6B column equilibrated with 20 mM Tris-HCl, 1 mM EDTA, pH 8.0. The colored fractions were combined and concentrated to 5–10 ml with a Diaflo concentrator (YM-10 membrane, Amicon, Inc., MA). The concentrated eluate was dialyzed with three changes against the same Tris-EDTA buffer with pH increased to 8.8. The solution was applied to the same column equilibrated with this buffer, and the colored fractions were concentrated again to 5–10 ml

and dialyzed further against 10 mM Tris and 0.5 mM EDTA at pH 9.8 for 36 h with 3 buffer changes. The recombinant Hbs were eluted with the same buffer containing 0.25 M NaCl. The buffers and solutions were kept saturated with CO. The final purified recombinant Hbs were stored at -80 °C.

Amino Terminus—Amino acid sequencing at the University of Texas Microanalysis Center showed a quantitative yield of proline in the recombinant Hb. The amino-terminal peptidase evidently removed all the methionine. Prior studies (25) showed no evidence in the native Hb for the formylation found in the Hb of the closely related *L. fluviatilis* (26).

Sedimentation Equilibrium—The CO-saturated recombinant Hbs were converted to HbO₂ with light (Sungun, Sylvania) and O₂ at 4 °C, diluted to ~18 μ M with 0.1 M phosphate buffer of pH 6.0, 6.5, and 7.5, and dialyzed overnight against this buffer. The dialyzed samples (100 μ l) were flushed with N₂ and equilibrated for ~1 h in an anaerobic chamber; then sodium dithionite (Miles Platting, Manchester, United Kingdom) was added to a concentration of 2 mg/ml, the same concentration used by Andersen (12). Double-sector Epon charcoal-filled centerpieces with quartz windows were used in sedimentation equilibrium experiments at 20 °C with a Beckman XL-A analytical ultracentrifuge³ equipped with an An60Ti rotor and a photoelectric scanner. The Epon cells were evacuated in the entering chamber for the anaerobic chamber and then remained in the chamber about 1 h. Initial experiments with 200- μ l samples required 44 h to reach equilibrium; 100- μ l samples were used subsequently to reduce the equilibration time. The experiments were performed with an initial rotor speed of 24,000 rpm for 1 h followed by 16,000 rpm until equilibrium was reached. The averages of five spectra were recorded from 300 to 650 nm at one radial position at the start and at the end. The averages of 20 radial scans at 430 and 560 nm with a step size of 0.001 in absorbance were obtained after equilibrium was reached. Duplicate scans at 430 nm 3–4 h apart were overlaid to determine when equilibrium was reached (~22 h for a 100- μ l sample).

The spectra at the start and end of an experiment showed maxima near 430 and 560 nm. The data were fitted by nonlinear least squares (27) to a monomer-dimer self-association model according to the equation,

$$A_{r,\text{total}} = e^{\ln A_0 + \frac{(1-v\rho)\omega^2}{2RT} M(r^2 - r_0^2)} + e^{[2 \ln A_0 + \ln K + \frac{(1-v\rho)\omega^2}{2RT} 2M(r^2 - r_0^2)]} + E \quad (\text{Eq. 1})$$

where A_r = the absorbance at radius r ; M = the monomer molecular weight, taken to be 16,898 from the sequence of PMII (19); v = the partial specific volume, calculated from the amino acid composition to be 0.742 ml/g (28); ρ = the solvent density; ω = the angular velocity, r = the radius; r_0 = the reference radius; E = the baseline offset; K is the monomer-dimer association constant. The buffer densities were calculated by the procedure of Laue *et al.* (29) to be 1.00849, 1.00943, and 1.01199 g/ml for 0.1 M phosphate of pH 6.0, 6.5, and 7.5, respectively. The absorbance of the reference sector at each radial position was subtracted from the absorbance of the sample sector to give $A_{r,\text{total}}$. This was necessary because the absorbance of the reference sector increased

³ The Beckman Optima XLA analytical ultracentrifuge is a component of the Center for Macromolecular Design of Texas A&M University, College Station, TX. Acquisition of the instrument was supported in part by grants from the National Science Foundation and the State of Texas.

TABLE III
Summary of sedimentation equilibrium data for the deoxygenated hemoglobins at 20 °C

Model	Hemoglobin	$K_{2,1}$ (μM) ^a			H ⁺ /heme ^c
		pH 6.0 ^b	pH 6.5 ^b	pH 7.4 ^b	
	Hemolysate	1.22 ± 0.20	9.2 ± 1.3	73 ± 6	0.62
	Hemolysate (12) ^d	1.86	4.75	122	0.66
	RecombinantHb	1.60 ± 0.02	5.3 ± 2.6	72 ± 24	0.59
$\alpha_1\beta_2$	D112N	1.49 ± 0.02	10.4 ± 0.1	127 ± 47	0.68
$\alpha_1\beta_2$	E50Q	3.67 ± 0.03	23.1 ± 1.9	M ^e	0.78
E/F	H73Q	25 ± 14	M ^e	M ^e	
E/F	K93E	3.1 ± 1.4	9.5 ± 2.0	M ^e	0.48
E/F	K93E/E31K	M ^e	M ^e	124 ± 24	
E/F	E75Q	3.43 ± 0.03	15.9 ± 1.8	56.4 ± 7.1	0.42
E/F	N79H		M ^e	M ^e	
E/F	N79D	M ^e		M ^e	
E/F	Y30H	M ^e	M ^e	M ^e	

^a $K_{2,1}$ is the equilibrium dissociation constant for the reaction of dimer to monomer. Values of $K_{2,1}$ were obtained by nonlinear least squares fitting to a monomer-dimer self-association model as described under "Materials and Methods."

^b See discussion of pH under "Materials and Methods."

^c Protons released per heme on dimer dissociation, calculated by linear regression from $1/2(\Delta\log K_{2,1}/\Delta\text{pH})$, for the pH values indicated. The estimated uncertainty in H⁺/heme is ±0.1.

^d Values calculated from the equation $K_{2,1} = K_d((K_p + H)/(H))^2$ from Andersen (12), where K_d is the dimer-monomer dissociation constant, 1 μM , for the protonated forms and K_p is the protonic dissociation constant, 0.4 μM , as estimated by Andersen.

^e M signifies that self-association was not measurable. These data were fitted with a single exponential to estimate the molar mass. The mean molar mass in twelve experiments with mutant Hbs which did not appear to form dimers under the conditions shown was $16,462 \pm 394$. This is 2.6% lower than the value based on structure, 16,899. This difference could be caused by an error of $-0.004 \text{ cm}^3/\text{g}$ in the partial specific volume used, 0.742 cm^3/g . Interestingly, a similar discrepancy exists in human Hb, where the value from amino acid composition is $\sim 0.745 \text{ cm}^3/\text{g}$ (29), but the measured value is about 0.004–0.005 cm^3/g higher (28).

about 0.002 per 0.1 cm increase in r except at the extremes where the absorbance was higher. The reasons for this variation in the reference sector are not known. The reference radius, r_0 , was chosen at or just below the meniscus in the sample sector. The least-squares fitting of the data to Equation 1 determined the best values of three parameters: A_0 , K , and E . A_0 and A_0^2K are the contributions of the monomer and dimer, respectively, to the total absorbance, corrected for the offset, E . The fitting gives the association constant in absorbance units which was converted to M^{-1} units by the relation $K_{1,2}$ (units, M^{-1}) = K_{abs}/ϵ , where the extinction coefficient, ϵ , for deoxy-Hb at 560 nm was measured to be $12.9 \text{ mm}^{-1} \text{ cm}^{-1}$ and the path length, l , in the centerpiece is 1.2 cm. The extinction coefficient was determined by measuring the absorption spectrum after determining the heme content by the alkaline hematin method (30).

Methemoglobin and Effects of Dithionite—The initial equilibration time of 44 h with 200- μl samples at pH 6.0 resulted in some metHb formation which caused the calculated dimer-monomer dissociation constant to be spuriously high because metHb is monomeric. However, subsequent measurements with a 100- μl sample did not show metHb at pH 6.0, and no measurable metHb was observed at pH 6.5 or 7.5. None of the spectra showed increased absorption at 630 nm as would be expected for metHb; the characteristic peaks of deoxy-Hb near 430 and 560 nm were observed. The quality of these spectra was not, of course, the same as with a stationary spectrophotometer so that any metHb less than about 5% would not be detected because of intrinsic noise. The great molar excess of dithionite should be sufficient to ensure reduction of any metHb.

The presence of oxygen was minimized by the use of an anaerobic chamber (Model HE-453-2 VAC, Atmospheres, Hawthorne, CA) of $\sim 1,200$ liters through which a constant stream of argon flowed. The argon was recycled through a palladium catalyst system that maintains the O_2 content below about 5 ppm. The solid dithionite was added in the chamber to an *already* deoxygenated buffer solution. An aliquot of the latter was added to a previously nitrogen-equilibrated Hb solution.

The possibility has been investigated that O_2 might come from the outgassing of the charcoal-filled Epon centerpieces during the ultracentrifugation. Control experiments were performed in which a dithionite-containing buffer solution, prepared anaerobically, was exposed to three charcoal-filled Epon centerpieces for 24 h in one anaerobically sealed glass container. The ratio of Epon surface area to buffer corresponded to that in the Hb-containing sector during ultracentrifugation. A similar quantity of dithionite-containing buffer was placed in a glass tube and sealed for 24 h. The change in pH of the Epon-exposed dithionite buffer compared with the buffer in the glass tubes was -0.01 at pH 6, 0.00 at pH 6.5, and -0.10 at pH 7.5. These results indicate that a small amount of outgassing of O_2 from the Epon cells does occur, but that the pH is measurably affected only at pH 7.5, not at pH 6.0 or 6.5.

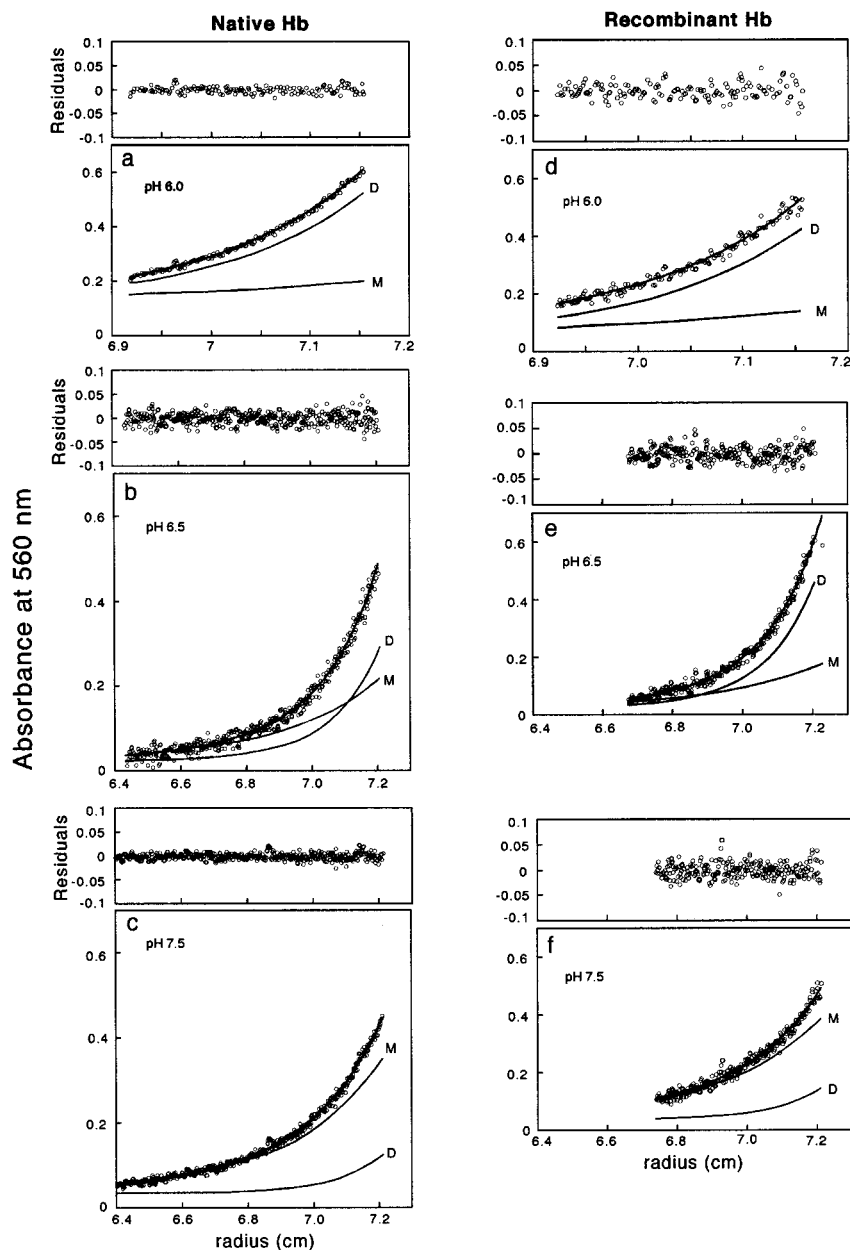
This difference can be explained by the oxidation of dithionite to form the bisulfite ion, HSO_3^- , which dissociates to SO_3^{2-} with a pK of 6.9 (31). Thus, the HSO_3^- would be 80% dissociated at pH 7.5, but only 11% at pH 6.0, so that a significant pH effect would not be observed at the lower pH. We have investigated the effect of the small pH change at pH 7.5 on the experimental determination of the number of protons released per dimer dissociated (see "Results"). The effect is an increase in protons released of only ~ 0.03 . The calculated values of protons released per dimer dissociated in Table III include this correction. There was also a small drop of -0.03 in pH upon addition of the dithionite to the buffer, but since this was not pH-dependent, it had no effect on the calculation of protons released.

Presence of Tetramers—The sedimentation data have been analyzed entirely in terms of a monomer-dimer association (Equation 1). Although self-association of deoxy lamprey Hbs to tetramers does occur (8, 11, 13), the 5 and 15 μM (heme) concentrations used in the present experiments preclude significant effects of higher-order association. Doi *et al.* (13) calculated the monomer-dimer and dimer-tetramer association constants to be $8.1 \times 10^4 \text{ M}^{-1}$ and $6.5 \times 10^3 \text{ M}^{-1}$, respectively, at pH 5.9, 20 °C. Calculations with these values suggest that tetramers should comprise $<0.2\%$ of the deoxy-Hb at 5 μM and $<2\%$ at 15 μM . The contribution of tetramers would be even smaller at higher pH values. Use of Andersen's (12) estimate for the dimer-tetramer association constant gives even lower quantities of tetramers. All the sedimentation data on associating systems analyzed in the present experiments could be fitted with a monomer-dimer model.

Oxygen Binding—Oxygen equilibria were measured by the method of Imai (32) at 20 °C with a Shimadzu spectrophotometer and a Keithly model 485 picoammeter. The optical path length of the Imai cell was 10.4 mm. All the Hb solutions contained the metHb reductase system of Hayashi *et al.* (33). After a complete deoxygenation curve (absorbance at 430 nm *versus* pO_2) was recorded, the nitrogen passing over the solution was replaced by 20% oxygen, and reoxygenation was recorded. The deoxygenation curves were used for all calculations. Spectra were recorded before deoxygenation and after reoxygenation. The oxygenation end points were obtained by extrapolation as described by Imai (32).

Amperometric Titrations—An hemolysate of lamprey red cells was dialyzed overnight against glass-distilled water and then made 0.1 M in phosphate, pH 7.3, and centrifuged to remove any precipitate. The clear hemolysate was titrated with HgCl_2 as described previously (34). Titrations were performed under either helium or carbon monoxide and with or without 8 M urea at 25 °C. The concentration of Hb was determined by measuring the O_2 liberated upon reaction with $\text{K}_3\text{Fe}(\text{CN})_6$ in a standard Warburg apparatus (35). These experiments were performed by A. F. R. in 1959–1960.

FIG. 1. Sedimentation equilibria of hemolysate and recombinant Hb (rHb). Panels a-c, hemolysate at pH 6.0, 6.5, and 7.5, respectively. Panels d-f, recombinant Hb at pH 6.0, 6.5, and 7.5, respectively. The curves shown through the data are those calculated by fitting to a monomer-dimer model as described in the text. Residuals are shown in the upper panels. Curves D and M show the contributions of dimer and monomer, respectively, to the total absorbance. The curves all start at the reference radius, r_0 .



RESULTS AND DISCUSSION

The goal of this study was to test and distinguish between three alternative models proposed by Honzatko and Hendrickson (15) and Perutz (16) for the interface in the dimer which forms upon deoxygenation of lamprey Hb. Although association beyond the dimer also occurs, the present experiments are confined to low protein concentrations where dimers predominate. The models for the intersubunit contacts are: (a) an " $\alpha_1\beta_2$ " interface corresponding to those of other vertebrate Hbs (15), (b) an E/F helix interface similar to that found in Hb II from the clam *Scapharca inequalvis* (15), and (c) Perutz' model, which also predicts the E helix contacts but invokes a special role for the distal histidine in forming an electrostatic link between monomers (16).

Hemolysate and Recombinant Hemoglobin

Fig. 1 compares the sedimentation equilibria for the unfractionated hemolysate from adult lamprey red cells and purified recombinant Hb, PMII', under anaerobic conditions. The data are satisfactorily fitted with a monomer-dimer model as described under "Materials and Methods." The residuals show no

systematic variation with radial distance. The data are summarized in Table III for the hemolysate, wild-type recombinant Hb (PM II'), designated rHb, and six mutants that show association from monomer to dimer, and three mutants for which any self-association was too small to be detected.

Comparison of the data for the hemolysate and rHb indicates that the pH dependence is almost identical despite differences in individual $K_{2,1}$ values. The value of $\frac{1}{2}(\Delta \log K_{2,1}/\Delta \text{pH})$ gives the number of protons released per heme for each dimer dissociated (36). The values for the two sets of data agree within 5% and are about 13% lower than those reported by Andersen (12). The differences between the hemolysate and rHb may reflect small differences in the multiple components present in the hemolysate.

The oxygen equilibrium curves of the hemolysate and the recombinant lamprey Hb are even more similar both in terms of the absolute values of P_{50} and n and their pH and concentration dependence (Fig. 2, Table IV). The presence of three major and additional minor components (18, 19) in the hemolysate has less effect on the oxygen binding parameters. However, on close examination, the data for the hemolysate indicate

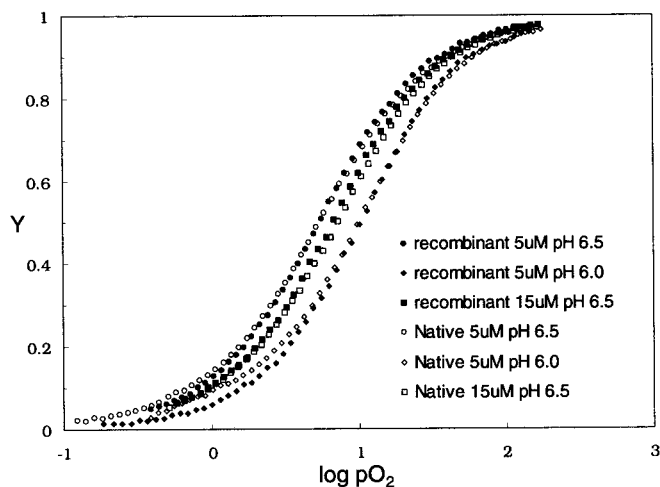


FIG. 2. Oxygen equilibria of hemolysate and recombinant Hbs (rHb).

the presence of a small quantity of Hb with higher oxygen affinity. The number of protons released per heme during dimer dissociation (Table III) is very similar to the number released per O_2 bound during oxygenation (Table IV). This finding is consistent with the conclusions of Andersen and Gibson (11) and Andersen (12) that the pH dependence of O_2 binding depends solely on the protons released as the result of dissociation of the dimer. Oxygenation of the monomer does not appear to be pH-dependent.

The oxygen equilibria for the hemolysate and recombinant Hb (Table IV) show a substantially lower O_2 affinity at pH 6.0 than that found in previous studies (11–13). The P_{50} values are 10 and 11.4 mm Hg at 5 and 15 μM Hb concentrations. These data are quite consistent with the sedimentation equilibria. Application of Equation 4 (see below) yields values at pH 6.0 of 57% and 72% dimer at 5 and 15 μM Hb, respectively. Dohi *et al.* (13), however, found that the $\log P_{50}$ values converged, independently of pH, to a single value of 0.63 ($P_{50} = 4.3$ mm Hg) at Hb concentrations $<5 \mu M$ where their analysis indicated that more than 90% of the Hb would be monomeric. This P_{50} , 4.3 mm Hg, would then correspond to the oxygen affinity of monomeric Hb under these conditions. The kinetic data of Andersen and Gibson (11) yield a similar value. They estimated the equilibrium dissociation constant for the monomer reaction, $HbO_2 \rightleftharpoons Hb + O_2$, to be 8 μM , which corresponds to ~ 4.8 mm Hg if we take 1 mm Hg pO_2 to give 1.68 $\mu M O_2$ in aqueous solution at 25 $^\circ C$ (37, 38).

The $\alpha_1\beta_2$ Model

Honzatko and Hendrickson (15) proposed four symmetry unique hydrogen bonds for an $\alpha_1\beta_2$ -like interface in the dimer of *Petromyzon* Hb:⁴ Glu⁵⁰(C6) Gln¹¹⁰(FG4), Asp¹¹²(G1) Tyr¹¹⁵(G4), Gln¹¹⁴(G3) Gln¹¹⁴(G3), and Gln¹¹⁴(G3) Tyr¹¹⁵(G4). The Asp¹¹²(G1) residues from each subunit would be pointing at each other. We tested this model with two mutations: Glu⁵⁰ \rightarrow Gln (E50Q) and Asp¹¹² \rightarrow Asn (D112N), thereby removing contributions by charged residues from the proposed interface.

The $K_{2,1}$ values for the D112N mutant do not indicate any major disruption of the dimer interface, and the number of protons released per mutant dimer dissociated is similar to that of the wild-type protein. The dimer-to-monomer dissocia-

tion equilibrium constant for the E50Q mutant is 2–4-fold greater than that of wild-type protein, but the value for H^+ released per heme is similar to that of the D112N mutant. Surprisingly, the E50Q mutation causes a 2-fold decrease in oxygen affinity (Fig. 3, Table IV). Heretofore, the only mechanism known for lowering the oxygen affinity of lamprey Hb has been dimerization, but the sedimentation data for this mutant show a modest decrease in dimer formation. The lowered O_2 affinity presumably reflects a conformational change at the active site.

Regardless of the exact interpretation, the functional effects of the D112N and E50Q mutations rule out the Honzatko and Hendrickson $\alpha_1\beta_2$ model. This model is also rendered unlikely by comparison of 10 amino acid sequences from 5 species of lamprey (18, 19, 40–42) which shows that the residues proposed for the $\alpha_1\beta_2$ model are not conserved at all, but that the residues proposed for the E/F clam model are conserved almost absolutely.

The E/F Clam Interface Model

Honzatko and Hendrickson (15) proposed a model in which there would be four major interactions in the dimer interface:⁴ Glu³¹(B3) Lys⁹³(EF7), Tyr³⁰(B2) Asp⁸³(E17), Glu⁷⁵(E9) Asn⁷⁹(E13), and Arg⁷¹(E5) Asp⁸³(E17). Six mutants were constructed to explore the importance of these possible interactions.

E/F K93E—On the basis of the E/F clam model for the interface, this mutation would be expected to abolish dimerization by electrostatic repulsion between two adjacent glutamyl residues. The sedimentation data at pH 6.5 indicate that the substitution causes a 2-fold increase in the value of $K_{2,1}$, the dissociation constant at both pH 6 and 6.5 (Table III). The Bohr effect is reduced slightly.

E/F, A/B Double mutant E31K/K93E—This construction simply reverses the positions of glutamyl and lysyl residues and should have little or no effect, if the E/F clam model were correct. However, this mutation abolished self-association entirely at pH 6.0 and 6.5. This result implies a crucial role for residue Glu³¹(B2) in the dimer interface because the K93E substitution has relatively little effect by itself. Surprisingly, the sedimentation results at pH 7.5 (Table III) indicated nearly normal behavior. A possible reason for this is discussed below.

A/B Y30H—The E/F clam model suggests that this mutation should strengthen the hydrogen bonding between B2 and E17 residues. However, the actual effect was to prevent self-association. We conclude that both Tyr³⁰ and Glu³¹ near the AB corner must form part of the interface. The oxygen affinity of the Y30H mutant is close to the estimates by Dohi *et al.* (13) and Andersen and Gibson (11) for the pH-independent oxygenation of monomers, 4.3–4.4 mm Hg (Table IV).

N79D (E13)—The E/F clam model suggests that this substitution should prevent self-association by electrostatic repulsion. The centrifugation results show that the substitution does prevent association, a finding consistent with an important role for Asn⁷⁹ in the interface (Table III).

N79H (E13)—The E/F clam model suggests that this mutation should increase the association by providing a stronger hydrogen bond donor to Glu(E9). However, the mutant Hb does not associate measurably. Similarly, the O_2 equilibrium curve of the mutant Hb shows a 3–6-fold increase in O_2 affinity and a loss of the Bohr effect at 5 μM concentration with respect to the wild-type protein (Fig. 4, Table IV). The oxygen affinities of the two mutant Hbs, N79H and N79D, are higher than those for any of the other mutants or that estimated for the monomer. The results show that Asn⁷⁹ is indeed important in the interface, but that the actual interactions are evidently not those

⁴ Helix designations vary somewhat in different Hbs according to where the helix starts. Here we use the designations and alignment given in Ref. 39 for comparative purposes.

TABLE IV
Summary of oxygen equilibrium data for mutants of lamprey hemoglobin

Hemoglobin	Concentration	pH 6.0		pH 6.5		H ⁺ released/heme ^a
		P_{50}	n_{\max}^b	P_{50}	n_{\max}^b	
Hemolysate	5 μM	9.1	1.15	5.2	1.13	0.48
	15 μM			6.8	1.20	
Recombinant Hb	5 μM	10	1.30	5.4	1.20	0.54
	15 μM	11.4	1.15	6.4	1.22	
Y30H (B2)	15 μM	4.7	0.97			0.50
E50Q (C6)	5 μM	19	1.17	10	1.21	
H73Q (E7)	5 μM	2.6	0.94	2.6	1.01	0
	15 μM	3.2	0.99	2.8	1.02	
E75Q (E9)	5 μM	6.7	1.23	5	1.22	0.25
	15 μM	8.9	1.27			
N79H (E13)	5 μM	1.7	1.04	1.6	0.98	0
N79D (E13)	15 μM			1.6	1.0	
Hemolysate (Ref. 6)	2 mM		pH range 6.3–7.4			0.69
Hemolysate (Ref. 7)	15 mM		pH range 6.3–7.7			

^a Calculated from $-\Delta\log P_{50}/\Delta\text{pH}$.

^b The calculated maximal value of the Hill coefficient.

^c The value given is from the regression slope. The value of $\Delta\log P_{50}/\Delta\text{pH}$ actually increases from 0.57 (pH 6.3–6.8) to 0.73 (pH 6.8–7.3) and 0.97 (pH 7.3–7.7).

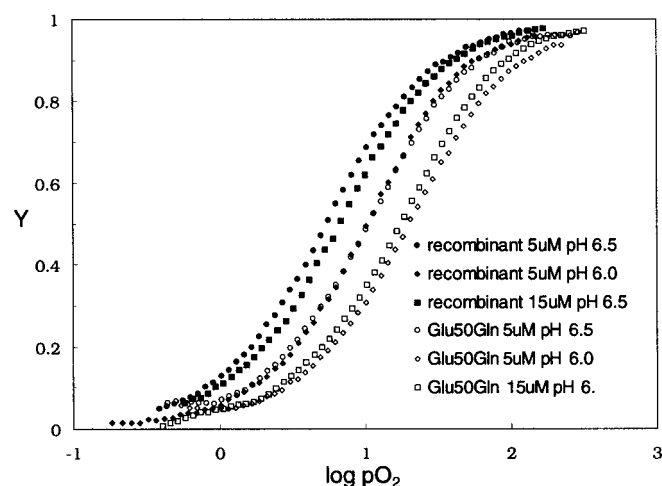


FIG. 3. Oxygen equilibria of the mutant, E50Q, compared with the equilibria for rHb.

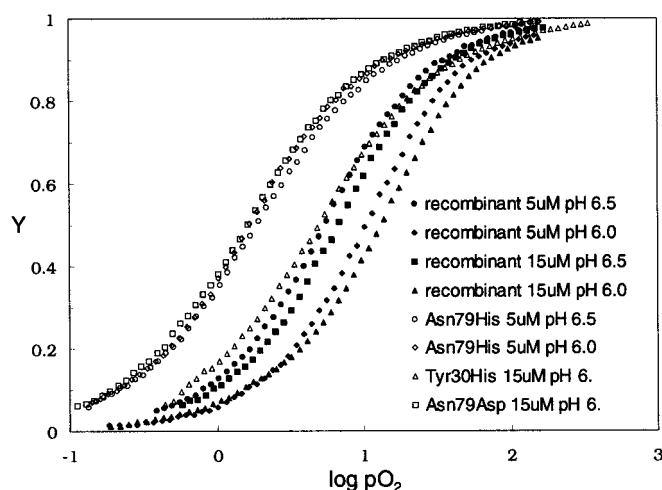


FIG. 4. Oxygen equilibria of the mutants N79D, N79H, and Y30H compared with oxygen equilibria for rHb.

suggested by the clam model.

E75Q (E9)—Sedimentation equilibria indicate that this substitution causes a significant decrease in the pH dependence of $K_{2,1}$ (Fig. 5, Table III). Similarly, the pH dependence of O₂ binding also decreases (Fig. 6, Table IV). These results provide

strong evidence that Glu⁷⁵ is responsible for at least part of the Bohr effect.

The Distal Histidine Model

Perutz (16) suggested that the distal histidine swings out of the heme pocket upon deoxygenation of the monomeric Hb to form an electrostatic link with a carboxyl group of another molecule. Protonation of the distal histidine upon deoxygenation and dimerization would explain the Bohr effect. Perutz suggested that the model could be tested by making the distal histidine mutant, H73Q. Sedimentation analysis measurements (Fig. 7, Table III) show that this mutation does indeed abolish measurable self-association at pH 6.5 and causes a 15–16-fold decrease in association at pH 6.0. The oxygen affinity is increased 3.5–4.0-fold (Fig. 8, Table IV), and a Bohr effect is not measurable at a protein concentration of 5 μM . This shift parallels the results of the sedimentation equilibria in which a low degree of self-association was observed ($K_{1,2} \approx 0.04 \mu\text{M}^{-1}$ compared with $0.63 \mu\text{M}^{-1}$ for rHb). These results are qualitatively consistent with Perutz' model. However, as described below, the effect of the substitution appears to be indirect.

Cooperativity and Oxygenation

The data on the oxygen equilibria at pH 6 and 5 μM for rHb and the mutant H73Q in Fig. 8 are transformed into a Hill plot in Fig. 9a. The slope, n , for the rHb data increases with oxygenation from 1.0 to a maximal value of ~ 1.3 at 70–80% oxygenation and then decreases to 1.0 (Fig. 9b). The asymmetric variation of n with y (Fig. 9b) closely resembles the n versus y relationship for human hemoglobin Kansas (43) which undergoes a similar oxygenation-dependent dissociation, albeit from tetramer to dimer. Hill plots (not shown) for the oxygen equilibria of native lamprey Hb and mutants E50Q and E75Q are similar to those of rHb, and Hill plots for the non-associating mutants resemble those for H73Q. The Hill plots for O₂ equilibria of rHb and the associating mutants at pH 6.0 and 6.5 are similar. Quantitative analyses of these equilibria in terms of oxygenation models will require the use of higher concentrations than those used here.

Structural Basis for the Bohr Effect

The recent determination of a crystal structure of the deoxy lamprey Hb (17) shows a remarkable cluster of four glutamyl residues in the dimeric interface (Fig. 10). This cluster has two Glu⁷⁵-Glu³¹ pairs in which the carboxyl oxygens are only 2.7 Å

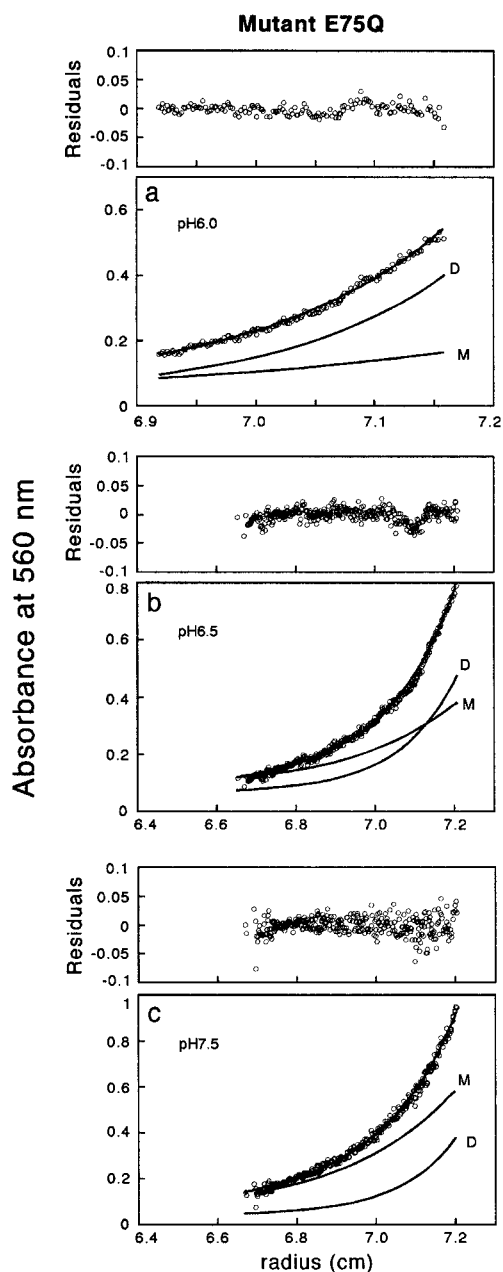


FIG. 5. Sedimentation equilibria for the mutant Hb E75Q. Panels a-c are for experiments at pH 6.0, 6.5, and 7.5, respectively. Curves *D* and *M* show the contributions of dimer and monomer, respectively, to the total absorbance. All the curves start at the reference radius, r_0 . Residuals are shown in the upper panel.

apart, as expected for hydrogen bonds. Arg⁷¹ is also 2.7 Å from Glu³¹. We consider here how these residues are related to the functional properties.

pK Shifts

Wald and Riggs (6) and Briehl (7) found that approximately 0.7 protons were released per O₂ bound from the value of $\Delta \log P_{50}/\Delta \text{pH}$ measured at millimolar Hb concentrations. The release of protons upon oxygenation reflects a shift in pK of acid groups. Wyman (44) showed that the minimal change in pK for a Hb with a single linked acid group per heme is given by the expression,

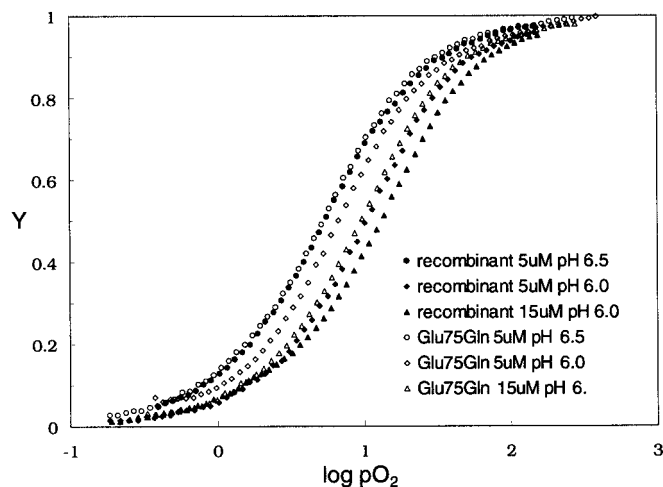


FIG. 6. Oxygen equilibria of the mutant Hb E75Q, compared with rHb.

$$\Delta \text{pK} = 2 \log \frac{1+r}{1-r} \quad (\text{Eq. 2})$$

where $r = \Delta \log P_{50}/\Delta \text{pH}$. If $r = 0.7$, the calculated $\Delta \text{pK} = 1.5$. If we assume glutamyl residues to be the Bohr groups on the basis of the x-ray structure and take the intrinsic pK of the γ -carboxyl of glutamate in the polypeptide to be 4.51 (45),⁵ then the pK of the Glu in deoxy lamprey Hb would rise to 6.0, identical to the value estimated by Andersen and Gibson (11).

The crystal structure (17) indicates that the formation of the dimer interface requires the cooperative uptake of two protons, one for each Glu-Glu pair, to compensate for the electrostatic repulsion.⁶ The shift in pK of glutamyl residues occurs primarily because of the effect of the electric field of one glutamyl carboxyl group on the ionization of the second glutamyl carboxyl. The pK shift can be readily estimated for the simplifying condition that no other groups are involved. Of course, the actual environment will be more complex. However, the following considerations show that a pK shift of 1.5 requires only a minor change in the dielectric constant. The pK shift caused by the electric field of a single neighboring group can be estimated from the relationship (46),

$$\Delta \text{pK} = \frac{N\epsilon^2}{2.303 D r R T} \quad (\text{Eq. 3})$$

where N is Avogadro's number, ϵ is the charge of one electron, D is the dielectric constant, and r is the distance between the groups. If we take $r = 2.7$ Å from the x-ray data and $\Delta \text{pK} = 1.5$ from the oxygen equilibria, the equation is satisfied if the value for the dielectric constant, D , is reduced from 78.5 (pure water) to 60, a very modest reduction in an interface from which water is excluded.

⁵ This estimate is based on measurement at an ionic strength of 0.1 at 25 °C of the acid dissociation constant of *N*-acetyl-L-isoglutamine, the structure of which corresponds to a glutamate residue in a polypeptide chain, CH₃CONHCH(CH₂CH₂COO⁻)CONH₂. The sedimentation and oxygen equilibria were performed at 20 °C. This small temperature difference would cause a negligible increase in pK of ~0.01 if the ΔH° value for the ionization of the similar γ -carboxyl group of aspartate, 1110 cal/mol (46) is used.

⁶ Cooperative uptake was suggested by Antonini *et al.* (47) who found that the $\log P_{50}$ versus pH curves were so steep that no set of independent acid groups would explain the data, so they proposed a positive interaction.

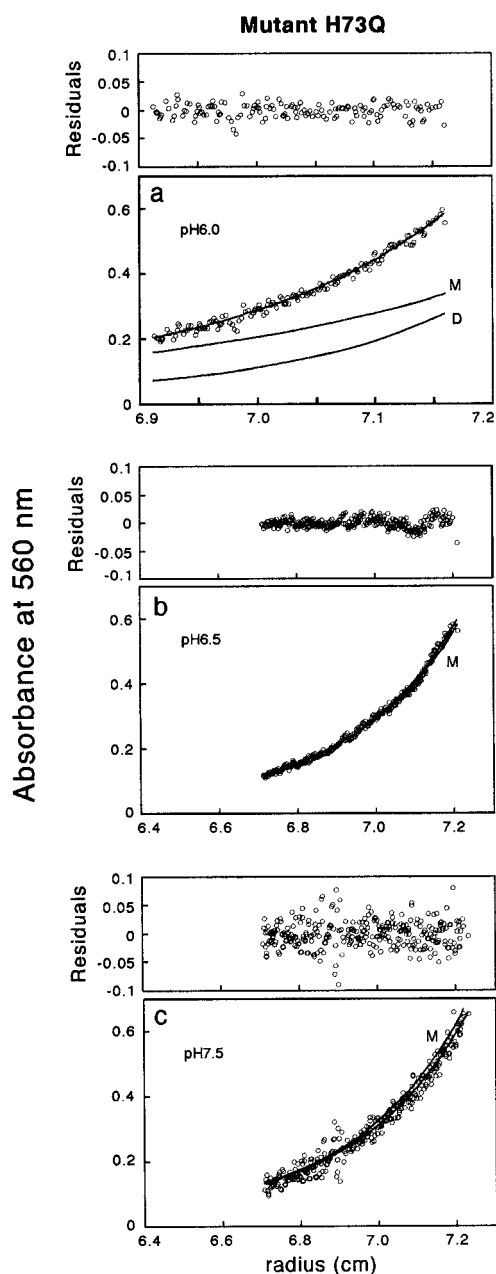


FIG. 7. Sedimentation equilibria of the mutant Hb, H73Q. Panels *a-c* are for experiments at pH 6.0, 6.5, and 7.5, respectively. The data for pH 6.0 are fitted to a monomer-dimer model, those for pH 6.5 and 7.5 were fitted with a single exponential. Residuals are shown in the upper panels. The fitted curves in *b* and *c* give the best fit values of the weight-average molar mass as 17,357 and 16,596 at pH 6.5 and 7.5, respectively, which do not differ significantly from the structural value of 16,899 used for curve *M* shown (see Footnote e, Table III). The curves start at the reference radius, r_0 .

Dependence of Sedimentation and Oxygen Binding

How can the results from sedimentation equilibria be related to those for oxygen binding? The present results (Tables III and IV) and those of Andersen and Gibson (11) indicate that the Bohr effect can be entirely accounted for by a mandatory protonation of one acid group per heme that accompanies the dimerization of deoxy-Hb. Thus, the number of protons released during oxygenation will be determined by the fraction, α , of the deoxy-Hb present as dimers. This fraction is given by the expression,

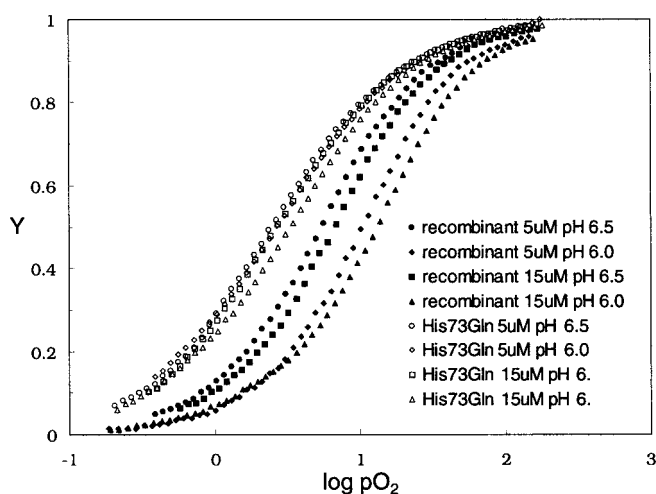


FIG. 8. Oxygen equilibria for the mutant Hb, H73Q, compared with data for rHb.

$$\alpha = 1 + \frac{1}{2KC} - \frac{1}{2KC} \sqrt{1 + 4KC} \quad (\text{Eq. 4})$$

where K is the monomer-dimer association constant and C the concentration of heme groups. At pH 6.0, $K_{1,2} \approx 6.25 \times 10^5 \text{ M}^{-1}$ for the wild-type recombinant Hb and $2.92 \times 10^5 \text{ M}^{-1}$ for the mutant E75Q. If $C = 5 \mu\text{M}$, then $\alpha = 0.57$ for the wild-type protein and 0.45 for E75Q. If two acid groups are present per dimer of wild-type protein, then 0.57 H^+ /heme would be released upon dimer dissociation, close to the value of 0.54 H^+ /heme released per O_2 bound, determined from the oxygen equilibrium curves (Table IV). If the mutant E75Q has only one acid group, then only 0.23 H^+ /heme would be released upon dimer dissociation, which is close to the value determined experimentally from the O_2 equilibrium curves, 0.25 H^+ per O_2 bound (Table IV).

Our correlation of the pH dependence of sedimentation and oxygen equilibria carries the tacit assumption that the self-association of HbO_2 is negligible. The sedimentation data of both Behlke and Scheler (8) and Dohi *et al.* (13) show that the self-association of HbO_2 will have no significant effect on our conclusions at the pH and low Hb concentrations used. In summary, the analysis supports the conclusion that two acid groups are present in the dimer of native or recombinant adult Hb and that one of these acid groups has been removed in the E75Q mutant and that one linked acid group remains in the E75Q mutant.

The interface in the x-ray structure of the deoxy dimer (Fig. 10) shows two pairs of the triad Glu³¹, Glu^{75'}, and Arg^{71'}. One proton between each Glu³¹ and Glu^{75'} pair will balance the charges. This arrangement accounts well for the Bohr effect as proposed (17) but suggests that the mutation E75Q should abolish the Bohr effect because Arg^{71'} is only 2.7 \AA from Glu³¹. This interaction would be expected to prevent Glu³¹ from being an effective Bohr group by itself because the electric field of Arg^{71'} would greatly lower the pK of Glu³¹. However, both the sedimentation and the oxygen equilibria show that a Bohr effect is still present in E75Q. Two ways out of this dilemma can be suggested. First, dimer formation might still require a proton between Glu³¹ and Glu^{75'} in the mutant. Glu³¹ would then no longer balance the change of Arg^{71'} so an anion would be needed. A difficulty with this proposal is that it involves the release of two protons per dimer, but this is not consistent with the experimental data. Examination of the orientation of Glu³¹ and Glu^{75'} in Fig. 10 suggests an alternative possibility. A relatively minor rearrangement would be sufficient to have

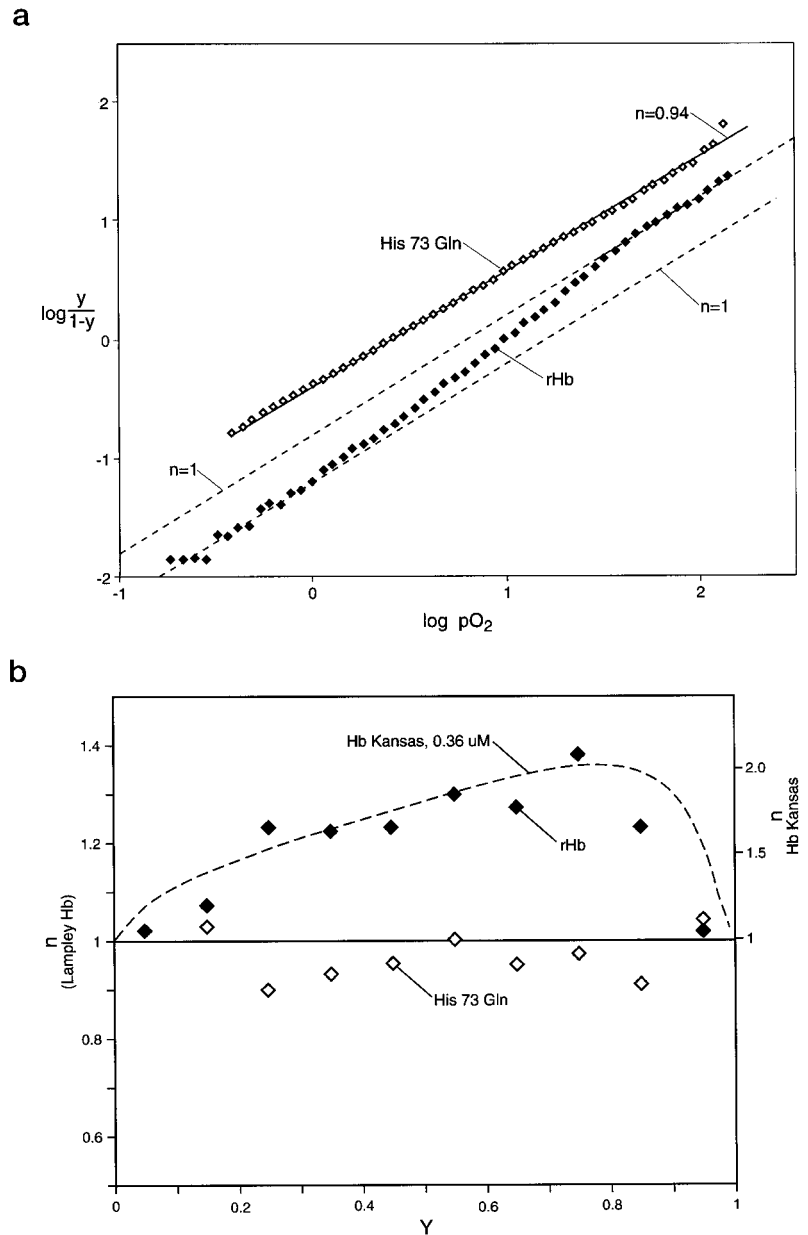
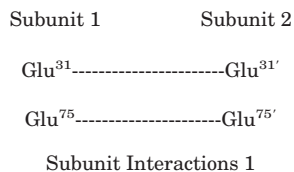


FIG. 9. *a*, Hill plots of the oxygen equilibria of rHb and the mutant H73Q both at pH 6.0 and 5 μ M; values are derived from the data in Fig. 8. *b*, variation of the Hill coefficient, n , with the degree of oxygenation, y , for the data shown in *a*. The dashed line is the variation of n with y estimated for the oxygen equilibrium of human Hb Kansas at 0.36 μ M (Fig. 3 of Ref. 43).

Glu⁷⁵ and Glu³¹ of each monomer subunit hydrogen-bonded to their counterparts in the other subunit,



This alternative arrangement would account for a Bohr effect in the E75Q mutant as due to protonation of the Glu³¹ . . .Glu^{31'} pair. However, this scheme still requires balancing the charge on Arg⁷¹ by anions. Such a structure seems plausible because at least four crystallographically distinct but similar structures of deoxy lamprey Hb have been observed (14). This suggests that several alternative conformations may occur under slightly different ionic conditions and that anions might have a physiologically important effect on the Bohr effect because of the proximity of Arg⁷¹ to Glu³¹.

The single mutant Y30H and the double mutant K93E/E31K both completely abolish the self-association of deoxy-Hb at

pH6.0–6.5. The effect of the double mutation can be attributed entirely to electrostatic repulsion between E31K and Arg⁷¹ because the K93E mutant by itself has relatively little effect. The observed nearly normal self-association at pH7.5 for the K93E/E31K double mutant can be attributed to the dissociation of a proton from Lys³¹ at this pH, thereby removing the repulsion. Arg⁷¹ would lower the pK of Lys³¹. Electrostatic repulsion by Arg⁷¹ could also explain the reduction of dimer formation by Y30H.

Bohr Effect at High Concentrations

Nikinmaa (48) has made an important, careful experimental analysis of Hb function within intact red cells of *L. fluviatilis*. He found that $\Delta \log P_{50}/\Delta pH = -1.03$ in terms of the intracellular pH. How well do the present Bohr effect results compare with this value? This, of course, requires a rather gross extrapolation. The rHb data, obtained at 5 and 15 μ M heme and at pH 6.0 and 6.5 (Table III) have been extrapolated to ~ 15 mM and pH ~ 7.8 (approximate red cell values (48)) with the application of Equation 4. The result is an apparent dimer proportion of 0.90. Thus, O₂ binding would cause the release of 1.8 H⁺ per

FIG. 10. Stereoview of the subunit interactions in the dimer of adult lamprey Hb, prepared from the coordinates of the x-ray structure (17) in the Protein Data Bank, PDB ID number 3lhb (MMDB ID: 12226).

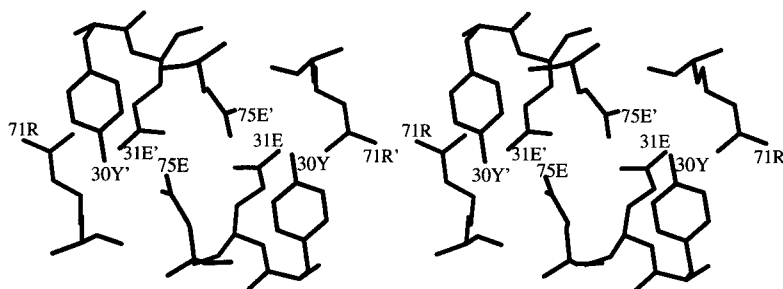


TABLE V
Mercuric ion titration of lamprey hemoglobin

^a Hb concentration, 1.13 mM on heme basis, buffer, 0.1 M phosphate, pH 7.3. Measurements were made at room temperature, ~25 °C.

Conditions ^a	Hg ²⁺ bound/heme
Deoxy-Hb under helium	0.06
Deoxy-Hb under helium, 8 M urea	0.70
CO-Hb	0.97
CO-Hb, 8 M urea	0.92

dimer or 0.9 H⁺/heme, close to the value reported by Nikinmaa. Briehl's results for 15 mM heme are also close to the intracellular value (see Table IV, Footnote c).

Role of the Distal Histidine

Several observations indicate that the structural changes on forming deoxy lamprey Hb are not confined to the interface. Heaslet and Royer (17) have suggested that the ligand-linked changes are all triggered, directly or indirectly, by the changes in the heme pocket associated with the movement of the distal histidine further into the pocket which reduces the accessibility of the heme iron to ligands by steric hindrance. Thus, the 3–5-fold increase in O₂ affinity caused by the H73Q mutant could be due both to the removal of steric constraints at the active site and to the disruption of the E-helix interface, facilitating dissociation into dimers and a loss of the Bohr effect.

Linkage of Deoxygenation with Non-interface Residues

It should be noted that the mutation of His(E7) to Gln in sperm whale myoglobin and in the R state α subunits of human hemoglobin causes decreases in O₂ affinity for both proteins, in contrast to what is observed for lamprey Hb. In mammalian Mb and Hb α chains, the distal histidine serves to stabilize bound O₂ by hydrogen bonding, and this favorable interaction is weakened by the glutamine replacement. In lamprey Hb dimers, the distal histidine appears to be inhibiting ligand binding by direct steric hindrance as is observed in human hemoglobin β chains, and this hindrance is alleviated significantly by glutamine substitution. At least two residues distant from the interface and heme pocket appear to be sensitive to oxygen binding: Cys¹⁴¹(H16) and Glu⁵⁰(C6).

The data in Table V show that ligated lamprey Hb binds a single Hg²⁺ ion per heme. The high affinity of the Hg²⁺ ions for –SH groups indicates that the single cysteinyl residue (residue 141) is the reacting group. Similarly, Allison *et al.* (49) found a single cysteine in lamprey Hb by titration with phenylmercuric hydroxide.⁷ Andersen and Gibson (11) also found a single reactive cysteine with the highly specific *p*-hydroxymercuribenzoate. The data (Table V) show that this cysteine becomes relatively inaccessible in deoxy lamprey Hb. Thus, the conformation of this part of the H helix must be sensitive to changes

in the heme pocket. Reciprocally, Andersen and Gibson (11) found that *p*-hydroxymercuribenzoate made the heme pocket more accessible to ligands. Rebinding kinetics after flash photolysis showed that the rates of reaction with CO and O₂ were doubled at high pH and that at low pH the reactions were biphasic with a slow reaction, indicating the presence of dimers. This result, along with the crystal structure, indicates that mercurial binding can affect the reactivity of the iron atom even though Cys¹⁴¹ is far removed from the dimer interface.

The E50Q substitution causes a 2-fold decrease in O₂ affinity (Fig. 3, Table IV). This result appears to be another reflection of conformational change in the globin that is not related to dimer formation. Indeed, the mutant exhibits 2–4-fold increased dissociation. A lowered O₂ affinity is difficult to understand because increased dissociation should increase O₂ affinity according to the mechanisms proposed. Further work is needed to understand the role of Glu⁵⁰(C6) in ligand binding.

Conclusions

The sedimentation and oxygen equilibria of mutants of lamprey Hb show that the E/F helices and the AB corners form the interface in the dimer of deoxy lamprey Hb. This result is completely consistent with the x-ray structure determined by Heaslet and Royer (17).

Dissociation of the deoxy dimer to monomers of lamprey Hb is accompanied by the release of two protons. Conversely, the formation of the dimer requires the uptake of two protons. The pH dependence of the dissociation accounts completely for the oxygenation Bohr effect. Thus, oxygenation of monomers in pH-independent.

The substitution E75Q halves the number of protons released both upon dimer dissociation and upon oxygenation. This result confirms the central role in the Bohr effect of the cluster of glutamyl residues found in the interface of the dimer by x-ray analysis.

Acknowledgments—We thank William E. Royer for valuable discussions, Thomas O. Baldwin for the use of laboratory facilities, David P. Giedroc for the use of an anaerobic chamber, and Wen-Yen Kao and Claire K. Riggs for providing help. We thank Stephen Raso and Jonathan M. Sparks for providing invaluable help in the ultracentrifuge experiments. J. S. O. and D. H. M. thank Dr. Satoru Unzai for building the Imai apparatus at Rice University and writing the operational software, Dr. Kiyoshi Nagai for providing parts and encouragement, and Dr. Kiyohiro Imai for other parts and technical help.

REFERENCES

- Qiu, Y., Raso, S., Mailet, D., and Riggs, A. F. (1998) *FASEB J.* **12**, A1427
- Svedberg, T., and Eriksson, I.-B. (1933) *J. Am. Chem. Soc.* **55**, 2834–2841
- Lankester, E. R. (1868) *J. Anat. Physiol.* **2**, 114–116
- Lankester, E. R. (1869) *J. Anat. Physiol.* **4**, 119–129
- Hoppe-Seyler, F. (1864) *Arch. Pathol. Anat. Physiol. Klinische Med.* **29**, 233–235
- Wald, G., and Riggs, A. (1951) *J. Gen. Physiol.* **35**, 45–53
- Briehl, R. W. (1963) *J. Biol. Chem.* **238**, 2361–2366
- Behlke, J., and Scheler, W. (1970) *FEBS Lett.* **7**, 177–179
- Behlke, J., and Scheler, W. (1970) *Eur. J. Biochem.* **15**, 245–249
- Riggs, A. F. (1998) *J. Exp. Biol.* **201**, 1073–1084
- Andersen, M. E., and Gibson, Q. H. (1971) *J. Biol. Chem.* **246**, 4790–4799
- Andersen, M. E. (1972) *J. Biol. Chem.* **246**, 4800–4806
- Doi, Y., Sugita, Y., and Yoneyama, Y. (1973) *J. Biol. Chem.* **248**, 2354–2363
- Hendrickson, W. A., Love, W. E., and Murray, G. C. (1968) *J. Mol. Biol.* **33**,

⁷ The value of 1.9 cysteines in denatured Hb reported by Allison *et al.* (49), inconsistent with subsequent sequence analysis, appears to have resulted from the use of dodecyl sulfate (400 mol/mol Hb).

- 829–842
15. Honzatko, R. B., and Hendrickson, W. A. (1986) *Proc. Natl. Acad. Sci. U. S. A.* **83**, 8487–8491
16. Perutz, M. F. (1989) *Quart. Rev. Biophys.* **22**, 139–236
17. Heaslet, H. A., and Royer, W. E. (1999) *Structure* **7**, 517–526
18. Hombrados, I., Rodewald, K., Neuzil, E., and Braunitzer, G. (1983) *Biochimie (Paris)* **65**, 247–257
19. Hombrados, I., Rodewald, K., Allard, M., Neuzil, E., and Braunitzer, G. (1987) *Biol. Chem. Hoppe-Seyler* **368**, 145–154
20. Rumen, N. M., and Love, W. E. (1963) *Arch. Biochem. Biophys.* **103**, 24–35
21. Shen, T.-J., Ho, N. T., Zou, M., Sun, D. P., Cottam, P. F., Simplaceanu, V., Tam, M. F., Bell, D. A., Jr., and Ho, C. (1997) *Protein Eng.* **10**, 1085–1097
22. Sarkar, G., and Sommer, S. S. (1990) *BioTechniques* **8**, 404–407
23. Datta, A. K. (1995) *Nucleic Acids Res.* **23**, 1187–1199
24. Barik, S., and Galinski, M. S. (1991) *BioTechniques* **10**, 481–491
25. Li, S. L., and Riggs, A. (1970) *J. Biol. Chem.* **245**, 6149–6169
26. Fujiki, N., Braunitzer, G., and Rudloff, V. (1970) *Hoppe-Seyler's Z. Physiol. Chem.* **351**, 901–902
27. Johnson, M. L., Correia, J. J., Yphantis, D. A., and Halvorson, H. R. (1981) *Biophys. J.* **36**, 575–588
28. Durschlag, H. (1986) in *Thermodynamic Data for Biochemistry and Biotechnology* (Hinz, H.-J., ed) pp. 45–128, Springer-Verlag, Berlin
29. Laue, T. M., Shah, B. D., Ridgeway, T. M., and Pelletier, S. L. (1992) in *Biochemistry and Polymer Science* (Harding, S. E., Rowe, A. J., and Horton, J. C., eds) pp. 90–125, Royal Society of Chemistry, Cambridge
30. Wolf, H. U., Lang, W., and Zander, R. (1984) *Clin. Chim. Acta* **136**, 95–104
31. Mayhew, S. G. (1978) *Eur. J. Biochem.* **85**, 535–547
32. Imai, K. (1981) *Methods Enzymol.* **76**, 438–449
33. Hayashi, A., Suzuki, T., and Shin, M. (1973) *Biochim. Biophys. Acta* **310**, 309–316
34. Riggs, A. (1960) *J. Gen. Physiol.* **43**, 737–752
35. Riggs, A. (1951) *J. Gen. Physiol.* **35**, 23–40
36. Wyman, J. (1964) *Adv. Protein Chem.* **19**, 223–286
37. Springer, B. A., Sligar, S. G., Olson, J. S., and Phillips, G. N., Jr. (1994) *Chem. Rev.* **94**, 699–714
38. Olson, J. S., and Phillips, G. N., Jr. (1997) *J. Biol. Inorg. Chem.* **2**, 544–552
39. Vandergon, T. L., Riggs, C. K., Gorr, T. A., Colacino, J. M., and Riggs, A. F. (1998) *J. Biol. Chem.* **273**, 16998–17011
40. Zelenik, M., Rudloff, V., and Braunitzer, G. (1979) *Hoppe Seyler's Z. Physiol. Chem.* **360**, 1879–1894
41. Hombrados, I., Vidal, Y., Rodewald, K., Braunitzer, G., and Neuzil, E. (1991) *Hoppe Seyler's Z. Physiol. Chem.* **372**, 49–56
42. Lanfranchi, G., Pallavicini, A., Laveder, P., and Valle, G. (1994) *Dev. Biol.* **164**, 402–408
43. Atha, D. H., Johnson, M. L., and Riggs, A. F. (1979) *J. Biol. Chem.* **254**, 12390–12398
44. Wyman, J. (1948) *Adv. Protein Chem.* **4**, 407–531
45. Nozaki, Y., and Tanford, C. (1967) *J. Biol. Chem.* **242**, 4731–4735
46. Edsall, J. T., and Wyman, J. (1958) *Biophysical Chemistry*, pp. 452–463, Academic Press, New York
47. Antonini, E., Wyman, J., Bellelli, L., Rumen, N., and Siniscalco, M. (1964) *Arch. Biochem. Biophys.* **105**, 404–408
48. Nikinmaa, M. (1993) *Resp. Physiol.* **91**, 283–293
49. Allison, A. C., Cecil, R., Charlwood, P. A., Gratzner, W. B., Jacobs, S., and Snow, N. S. (1960) *Biochim. Biophys. Acta* **42**, 43–48